J Incl Phenom Macrocycl Chem (2015) 82:135–143
DOI 10.1007/s10847-015-0473-3

ORIGINAL ARTICLE

Copper(II) and platinum(II) compounds with pyrene-appended dipicolylamine ligand: syntheses, crystal structures and biological evaluation

Ze-Li Yuan · Lei Wang · Xiao-Min Shen · Xiao-Qing Yang · Jian-Dong Huang · Gang Wei

Received: 16 December 2014 / Accepted: 2 January 2015 / Published online: 13 January 2015

Abstract The pyrene-appended dipicolylamine ligand (**L**) and its Cu(II) and Pt(II) compounds have been synthesized and characterized by elemental analysis, ^{1}H- and ^{13}C-NMR, HRMS, FT–IR and UV–Vis analyses. Furthermore, the crystal structures of $H_2L{\cdot}2ClO_4$, $[(CuLClO_4CH_3CN)ClO_4]$ and [(PtLCl)DMSO] (DMSO = dimethyl sulfoxide) have been determined by single-crystal X-ray diffraction. The antimicrobial activities of these compounds were determined towards Gram-positive (*Staphylococcus aureus* ATCC-25923) and Gram-negative (*Escherichia coli* ATTC-25922) strains of bacteria, as well as the fungal strain *Candida albicans* ATCC-10213, and the results were compared with those of **L** alone. The results of these experiments showed that the Cu(II) and Pt(II) compounds of **L** exhibited stronger antibacterial and antifungal activities than the ligand.

Keywords Dipicoclylamine ligand · Metal compound · Synthesis · Crystal structure · Antibacterial activity

Electronic supplementary material The online version of this article (doi:10.1007/s10847-015-0473-3) contains supplementary material, which is available to authorized users.

Z.-L. Yuan · L. Wang · X.-M. Shen · X.-Q. Yang · J.-D. Huang
College of Chemistry, Fuzhou University, Fuzhou 350108, Fujian, China

Z.-L. Yuan (✉)
School of Pharmacy, Zunyi Medical University, Zunyi 563003, Guizhou, China
e-mail: zlyuan@zmc.edu.cn

G. Wei (✉)
CSIRO Manufacturing Flagship, PO Box 218, Lindfield, NSW 2070, Australia
e-mail: gang.wei@csiro.au

Introduction

Although numerous remedial measures are currently available for the treatment of a wide range of human diseases and conditions, the search for new and improved therapeutic agents is a continuous and never ending process, and efforts in this area are continuing to increase [1–3].

A review of the literature for compounds claiming to elicit biological activities shows that uses of metal ions can be used as an effective strategy in specific therapeutic agents, such as DNA damaging agents in cancer chemotherapy, to enhance both the action and the efficacy of these agents following the coordination of a metal ion [4–6].

The most commonly used transition metals in the development of new anticancer and antibacterial drugs are platinum, palladium, rhodium, ruthenium, copper, silver and gold [7–11]. Furthermore, the effect of metal-based pharmaceuticals depends not only on the function of the metal but on the ligands themselves [12]. Polyaromatic hydrocarbons (PAHs) and their derivatives possess planar ring systems, which can intercalate with DNA to produce anticancer activity [13–15]. Several PAHs have been developed based on pyrene and chrysene derivatives such as (1-pyrenylmethyl)amino alcohol derivatives **I** and crisnatol **II** (770U82), which have progressed into different stages of clinical trials [16, 17]. The development of PAHs bearing a functional arm with additional hydrogen bond donor sites such as N and O atoms would allow for the formation of additional coordinate interactions between the PAH and a metal center, which would provide additional stability through chelation. Furthermore, additional coordinate interactions of this type would cause the metal-PAH system to adopt a rigid conformation, which would be better suited for the sustained release of the metal ions at the required site of action. Unfortunately, there have been very few studies

reported to date pertaining to the biological properties of metal-PAH compounds [18]. Based on the above consideration, and as a part of our ongoing research towards the development of an evaluation of novel metal–ligand compounds [19–21], we have prepared several new PAH-metal compounds and evaluated their activity as broad-spectrum bactericides. We have also tested the biological activities of a pyrene-appended dipicolylamine ligand as well as its Cu(II) and Pt(II) compounds against selected bacteria as potential antibacterial agents. In addition, we have described the synthesis, characterization and single crystal X-ray crystal structure of this ligand and its Cu(II) and Pt(II) compounds (**1** and **2**, respectively).

Experimental

Materials and measurements

All of the chemicals and reagents used in the current study were obtained from commercial sources as the analytical research (AR) grade and used without further purification. *N*,*N*-bis(2-pyridylmethyl)-amine (DPA) and *cis*-$PtCl_2(DMSO)_4$ were prepared according to previously described procedures [19, 22]. The ^1H and ^{13}C NMR spectra were recorded on an Agilent 400 DD2 spectrometer (Agilent, Palo Alto, USA) in DMSO-d_6, CD_3CN or $CDCl_3$ at ambient temperature. Chemical shifts (d) have been expressed in units of parts per million (ppm) relative to TMS, which was used as an internal reference. High resolution mass spectroscopy (HRMS) experiments were conducted on a time-of-flight Micromass LCT PremierXE Spectrometer (Mckinley, NJ, USA).Absorption spectra were recorded on a Cary50 UV–Vis spectrophotometer (Varian, Palo Alto, USA). Elemental (C, H, N) analyses were obtained with a Vario ELIII elemental analyzer (Elementar, WC, Heraeus, Germany). IR spectra were recorded on a Vary FT-IR 1000 FT-IR spectrophotometer (Varian, Palo Alto, USA) as KBr disks over the range of 400–4,000 cm^{-1}. The NMR, HRMS, FT-IR and physical properties data for each compound have been summarized below for each experiment. X-ray crystallography data were collected on a CCD SMART APEX diffractometer (Bruker, Karlsruhe, Germany) using graphite-monochromated Mo Kα radiation (λ = 0.71073 Å) at 293 K.

*Synthesis of 1-[bis(pyridine-2-ylmethyl)amino] methylpyrene (**L**)*

Pyrenecarboxaldehyde (1 mmol) and DPA (1 mmol) were placed in a round-bottomed flask followed by MeOH (5 mL), and the resulting mixture was irradiated at 300 W for 15 min at 60 °C. $NaBH_3CN$ (1.2 mmol) was then added to the reaction, and the resulting mixture was irradiated at 300 W for 30 min at 60 °C. The mixture was then cooled to ambient temperature and partitioned between a saturated aqueous solution of sodium carbonate and CH_2Cl_2. The organic phase was collected and the aqueous phases washed with CH_2Cl_2. The combined organic layers were washed sequentially with water and brine, and then dried over $MgSO_4$. The solvent was then removed *in vacuo* to give the crude product as a residue, which was washed with a small amount of MeOH before being recrystallized from a 1:1 (v:v) mixture of THF and EtOAc to give the desired ligand as a white powder. The isolated yield was 0.36 g (87 %). mp 178–180 °C. ^1H NMR (400 MHz, $CDCl_3$) δ: 3.92 (s, 4H), 4.38 (s, 2H), 7.09–7.26 (m, 2H), 7.47–7.52 (t, 2H, $J = 9.0$ Hz), 7.57–7.61 (m, 2H), 7.96–8.00 (m, 3H), 8.04–8.08 (t, 1H, $J = 7.2$, Hz), 8.10 (d, 2H, $J = 1.9$, Hz), 8.13–8.17 (dd, 2H, $J = 16.6$, 7.1 Hz), 8.35–8.37 (d, 1H, $J = 9.3$ Hz), 8.52–8.53 (d, 2H, $J = 7.6$ Hz). ^{13}C NMR (100 MHz, $CDCl_3$) δ: 156.05, 145.37, 145.31, 133.15, 133.0, 132.87, 129.01, 127.74, 127.30, 126.32, 124.75, 123.91, 123.50, 122.33, 121.46, 120.97, 119.84, 118.52, 57.00, 56.97, 53.67. HRMS (ESI–MS) calcd. for $C_{29}H_{23}N_3$ $[M+H]^+$: 414.1970, found *m/z*: 414.1956. Anal. calcd. for $C_{29}H_{23}N_3$: C 84.23 %, H 5.61 %, N 10.16 %, found: C 84.18 %, H 5.70 %, N 10.05 %. FT-IR (cm^{-1}) 3448, 3046, 2966, 2898, 2868, 1717, 1613, 1514, 1485, 1427, 1302, 1265, 1118, 787. UV–Vis (DMSO:CD_3CN = 1:1—v/v, 1.0×10^{-5} mol/L, λ_{max}/nm): 267, 278, 330, 347; Λ_m (DMSO:CD_3CN = 1:1—v/v, 1.0×10^{-5} mol/L, Ω^{-1}-mol^{-1} cm^2): 4.93. A single crystal for analysis by XRD was obtained via the vapor diffusion of diethyl ether into a concentrated acetonitrile and $HClO_4$ solution of the compound over 15 days at room temperature.

*Synthesis of [Cu**L**(CH$_3$CN)(ClO$_4$)]ClO$_4$·CH$_3$OH·2H$_2$O (**1**)*

To a solution of **L** (0.41 g, 1.0 mmol) in methanol(2 mL) at 60 °C, was added a solution of $CuClO_4 \cdot 6H_2O$ (0.27 g, 1.0 mmol) in acetonitrile(2 mL) with constant stirring on a magnetic stirrer plate. The resulting green solution was then stirred for an hour at 60 °C. The mixture was then concentrated under reduced pressure to precipitate the desired compound as a green solid, which was collected by filtration. The filter-cake was then washed sequentially with cold methanol and diethyl ether before being dried over anhydrous $CaCl_2$. The isolated yield of the dried product was 0.52 g (67 %). Anal. calcd. for $CuC_{31}H_{26}N_4O_4Cl \cdot ClO_4 \cdot CH_3OH \cdot 2H_2O$: C 48.96 %, H 4.37 %, N 7.14 %; found: C 48.79 %, H 4.38 %, N 7.21 %. HRMS (ESI–MS) calcd. for $CuC_{31}H_{26}N_4O_4Cl$ $[M+Na–ClO_4–CH_3OH–2H_2O]^+$: 639.0836, found *m/z*: 639.0707; FT-IR (cm^{-1}): 3445, 3046, 2915, 2847, 1597, 1582, 1487, 1428,

1376, 1241, 1103,762, 534. UV–Vis (DMSO:CD_3CN = 1:1—v/v, 1.0×10^{-5} mol/L, λ_{max}/nm) 268, 278, 329, 344. Λ_m (DMSO:CD_3CN = 1:1—v/v, 1.0×10^{-5} mol/L, Ω^{-1} mol^{-1} cm^2): 98.6. A single crystal for X-ray diffraction was obtained by slow recrystallization from a methanol solution of the compound.

*Synthesis of the compound [Pt(**L**)Cl]PF_6·DMSO·3CH_3OH (**2**)*

To a degassed solution of **L** (0.41 g, 1 mmol) and NEt_3 (0.31 g, 3 mmol) in methanol (10 mL) was added solid *cis*-[$PtCl_2(DMSO)_4$] (0.58 g, 1 mmol), and the resulting mixture was heated at reflux for 4 h under N_2. A small (5 mL) aliquot of a saturated solution of NH_4PF_6 was then added to the reaction, and the resulting solution was placed in a freezer overnight at −20 °C to aid the precipitation of the product. The resulting white precipitate was filtered, washed sequential with methanol and diethyl ether and then dried in an oven under vacuum at 40 °C. The dried product was isolated in a yield of 0.76 g (83 %). ^{1}H NMR (400 MHz, DMSO-d_6) δ: 2.64 (s, 6H), 3.34 (s, 12H), 5.03–5.07 (d, 2H, J = 15.8 Hz), 5.32–5.45 (m, 4H), 7.01–7.03 (d, 2H, J = 7.8 Hz), 7.29–7.32 (t, 2H, J = 6.6 Hz), 7.55–7.59 (m, 2H), 7.67–7.71 (m, 2H), 7.85–7.89 (t, 2H, J = 7.8 Hz), 7.92–7.94 (d, 2H, J = 8.3 Hz), 8.20–8.21 (d, 2H, J = 5.6 Hz), 8.34 (s, 1H), 8.79–8.81 (d, 2H, J = 8.9 Hz); Anal. calcd for $C_{29}H_{23}N_3ClPt$·DMSO·3CH_3OH: C, 49.90 %; H, 5.05 %; N, 5.14 %; found: C, 50.11 %; H, 5.01 %; N, 5.27 %. HRMS (ESI–MS) calcd. for $C_{29}H_{23}N_3ClPt$ $[M+H—DMSO—3CH_3OH]^+$: 644.1306; found *m*/*z*: 644.1196. FT-IR (cm^{-1}) 3463, 3046, 3018, 2926, 2360, 1602, 1463, 1445, 1075, 1072, 762, 560, 422. UV–Vis (DMSO:CD_3CN = 1:1—v/v, 1.0×10^{-5} mol/L, λ_{max}/nm) 271, 281, 335, 351. Λ_m (DMSO:CD_3CN = 1:1—v/v, 1.0×10^{-5} mol/L, Ω^{-1} mol^{-1} cm^2): 100.8. A single crystal for XRD analysis was obtained by the vapor diffusion of diethyl ether into a concentrated acetonitrile solution of the compound over a 7 day period at room temperature.

Crystal structure determination

Single-crystal X-ray diffraction data were collected on a Rigaku diffractometer (Bruker, Karlsruhe, Germany) with a Mercury CCD area detector (Mo Kα; λ = 0.71073 Å) at room temperature. Empirical absorption corrections were applied to the resulting data using the Crystal Clear program [23]. The structure was solved using direct methods and refined by the full-matrix least-squares on F^2 using the SHELXTL-97 program [24]. The metal atoms were located from the E-maps and the other non-hydrogen atoms were located in successive difference Fourier syntheses. All non-hydrogen atoms were refined anisotropically. The organic hydrogen atoms were positioned geometrically, while those of the water molecules were located using the difference Fourier method and refined freely. The C atoms of the pyrene ring were found to be disordered equally over two positions. PLATON/SQUEEZE was employed to remove the heavily disordered water molecules. Crystal data for L and its corresponding compounds **1** and **2** have been submitted to the Cambridge Crystal Structure Data Base (CCDC-1034520 for **L**, CCDC-1034521 for **1** and CCDC-1003396 for **2**).

In vitro antimicrobial assay

The antimicrobial activities of the ligand (L) and its Copper (II) and platinum (II) compounds **1** and **2** were tested against the Gram-positive and Gram-negative strains *Staphylococcus aureus* ATCC-25923 and *Escherichia coli* ATTC-25922, respectively, as well as the fungicidal strain *Candida albicans* ATCC-10213. All three of these strains were obtained from the Division of Microbiology, Department of Basic Medicine, Zunyi Medical University, China. These strains were grown in Mueller-Hilton agar at 37 °C for 24 h and the suspensions were prepared by matching a 0.5 McFarland standard [25, 26]. The test compounds were dissolved in DMSO and the resulting solutions were diluted with nutrient liquid medium to achieve a concentration of 10 %. The antimicrobial activities of these mixtures were tested by determining the minimum inhibitory concentrations (MICs) using the micro dilution plate method with resazurin.

Results and discussion

Synthesis

The ligand was synthesized according to the reductive amination method described in our previous work [19] using a monohydride source as the reducing agent, under microwave irradiation conditions (Fig. 1). Despite the steric bulk of the aldehyde groups, this synthetic approach was found to be more efficient than traditional methods when microwave irradiation was used as a heat source. Compound **1** was obtained in satisfactory yield (67 %) by the direct reaction of $Cu(ClO_4)_2$ with **L** in MeOH. Compound **2** was synthesized by the reaction of **L** with *cis*-[$PtCl_2(DMSO)_4$] in MeOH in the presence of NEt_3, which was added as a base, and NH_4PF_6, which was added as a precipitating agent. A variety of different reaction conditions were also investigated, and the results of these experiments revealed that the use of MeOH as the solvent and NEt_3 as the base gave the best yield of **2**. The success of these conditions was attributed to the reduction of the

Fig. 1 Scheme for synthesis of **L**

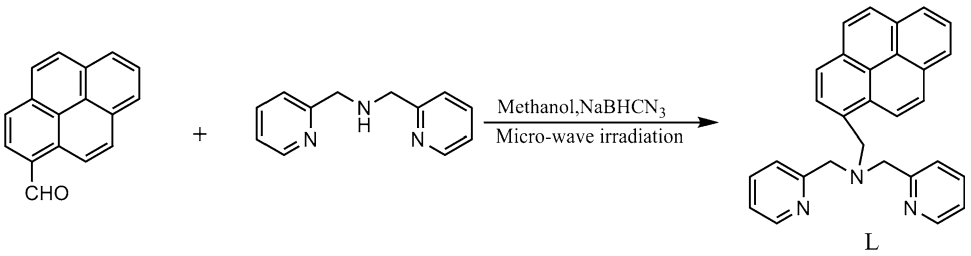

Pt(II) center by a combination of MeOH and NEt_3. Notably, compound **2** was not obtained when the reaction was conducted in acetonitrile, MeOH or ethanol with NaH as the base.

Characterisation and spectroscopic properties

Analytical results and some of the physical properties for **L** and its complexes with Cu(II) and Pt(II) (i.e., compounds **1** and **2**) are listed in the text. Compounds **1** and **2** were isolated as powered solids, which were soluble in DMSO, *N,N*-dimethylformamide (DMF) and acetonitrile. However, both of these compounds were insoluble in water. Compounds **1** and **2** were found to be stable ambient conditions, but decomposed without melting when they were heated up to 300 °C. Elemental analyses of these compounds revealed that compound **2** contained one molecule of DMSO *per* Pt(II) atom, which was consistent with a 1:1 ratio of compound species to solvate DMSO. The molar electric conductivity (Λ_m) values for compounds **1** and **2** were measured in a 1:1 (v/v) mixture of DMSO and CD_3CN and found to be typical of electrolytes [27], which indicated that these compounds are ionic in nature and undergo dissociation in solution.

Consideration of the ^{1}H NMR spectra of **L** and Pt(II) complex **2** (Figs. S1†, S3†) in $CDCl_3$ and DMSO-d_6 allowed for the elucidation of the specific binding mode of **L** to the metal ion. The aromatic portions of these spectra showed that the two pyridyl units were equivalent and that they had been shifted downfield with respect to the free ligand, which suggested that both of the pyridyl units were coordinated to the Pt(II) center. The methylene linker units also showed significant deviations from the chemical shifts of the free ligand. The pyrenyl methylene linker was observed as a doublet at 5.03–5.07 ppm. Two sets of resonance signals were assigned to the diastereotopic protons of the pyridyl methylene linkers; each of which integrated to two protons and had a coupling constant of approximately 16 Hz, which confirmed the existence of a geminal two-bond coupling interaction. The signals of belonging to the methyl protons of DMSO are worthy of special mention. The spectrum of **2** showed one DMSO signal (i.e., a singlet at 2.54 ppm), which was located in close proximity to the signal of the DMSO-d_6 NMR solvent. The signal at 2.54 ppm was positioned so close to the low-field side of the DMSO-d_6 quintet, that it was not possible to accurately integrate this signal without some interference from the NMR solvent. For this reason the NMR spectrum of **2** was also recorded in CD_3CN (Figs. 2, S4†), which showed a non-coordinated DMSO peak at 2.54 ppm. Based on this result, the signal at 2.54 ppm was assigned to non-coordinated DMSO.

The correct integration of the ^{1}H NMR spectrum in CD_3CN gave 6 protons for the coordinated DMSO in **2**, as required by the stoichiometry. This result was confirmed by XRD and elemental analyses of complex **2**, and the ratio of ligand molecules to non-coordinated DMSO molecules was therefore assigned as 1:1. The spectra of compounds **2** also show singlets at 3.34 ppm, assigned to CH_3OH.

The ^{13}C NMR spectra of **L** and **2** are shown in Figs. S2† and S5†, respectively. The assignments for these compounds were found to be in good agreement with the data for several other chelate compounds and Pt(II) sulfoxide compounds. The ^{13}C NMR spectrum of **2** revealed that the solvent (DMSO) signal was expanded with an additional signal at 40.44 ppm, which was positioned in close proximity to the lowest-frequency component of the septet (Fig. S5†). This signal was attributed to free (non-coordinated) DMSO. The intensity of the DMSO-d_6 signal should be distributed over seven lines and a signal of this type could be readily masked by noise under the conditions used in the current study.

HRMS analysis of **L** revealed the presence of a parent ion peak with an *m/z* value of 414.1956 (Fig. S6†), corresponding to the monoprotonated form of the parent compound. However, the dominant features in the mass spectra of compounds **1** and **2** (Figs. S7† and S8†) following their analysis by HRMS were the cationic fragment peaks with *m/z* values of 639.0707 and 644.1196, respectively, which were attributed to the intermediate compounds $[CuL(ClO_4)(CH_3CN{+}Na]^+$ and $[PtLCl{+}H]^+$. These peaks occurred as a consequence of ionization, which induced the loss of the DMSO, MeOH and PF_6^- ligands to form cationic fragments, and represents a common feature of the mass spectra of species of this type.

The FT-IR spectra of **L**and the corresponding Cu(II) and Pt(II) complexes **1** and **2** are shown in Figs. S9–11†. It is known that the $\upsilon_{(ClO_4^-)}$ stretching band appears at

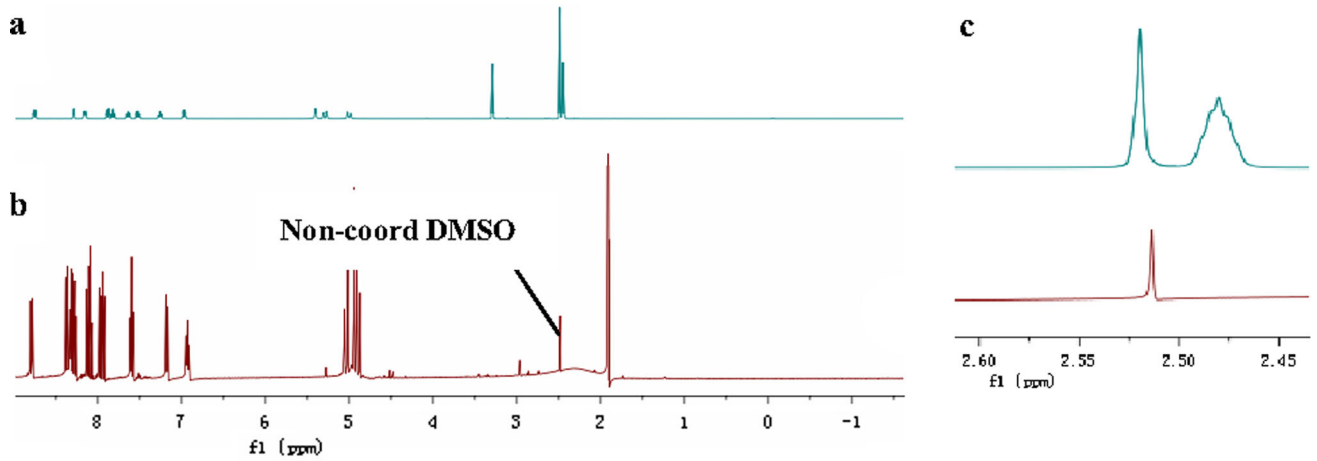

Fig. 2 ^{1}H NMR spectra of compound **2** with assignments: **a** in DMSO-d_6; **b** in CD_3CN; **c** magnification of the DMSO-d_6 peak in the range of 2.45–2.60 ppm. *up* in DMSO-d_6, *down* in CD_3CN

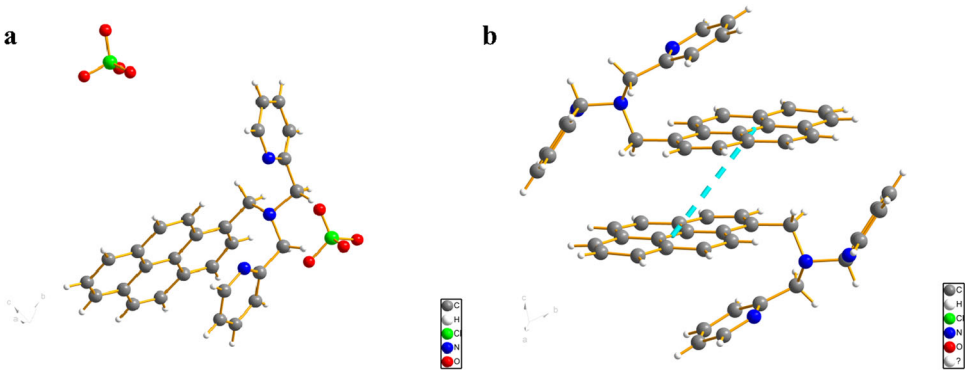

Fig. 3 **a** The asymmetric unit of **L**; **b** The π…π stacking interaction in **L**

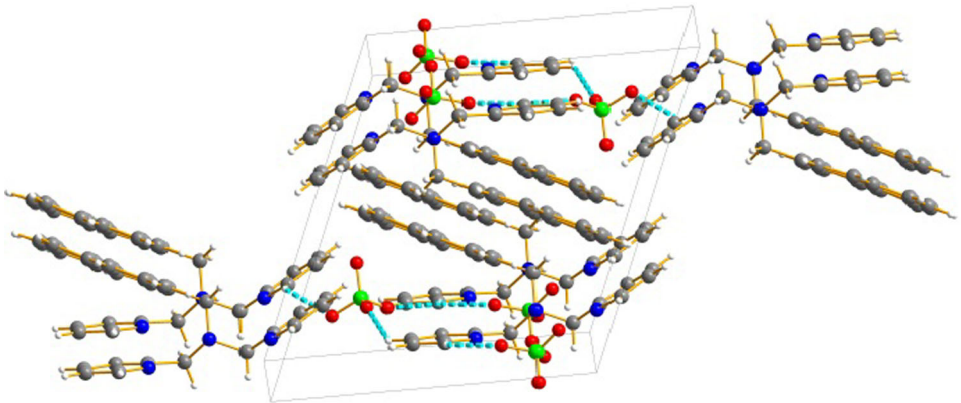

Fig. 4 The hydrogen bonds in **L**

1,103 cm^{-1} for **1** [28]. In addition, the $\upsilon_{(SO)}$ vibrations of solid-state free DMSO usually appear at 1,050–1,080 cm^{-1} in its FT-IR spectrum [29]. Based on these facts, it was possible for the band at 1,052 cm^{-1} in the FT-IR spectrum of compound **2** to be assigned to the $\upsilon_{(SO)}$ vibrations of the non-coordinating DMSO solvent molecule in **2**. Furthermore, the bands observed in the FT-IR spectra of **1** and **2** at 560, 524 and 422 cm^{-1}, were not observed in the spectrum of the free ligand, and could therefore be attributed to the metal-nitrogen stretching vibrations of **1** and **2** [30–32].

The UV–Vis spectra of **L**, **1** and **2** are shown in Fig. S12†. The absorption spectra of compounds **1** and **2** closely resembled that of the free ligand. Furthermore, the spectra of **1** and **2** were dominated by ligand-based π–π*

transitions at 267–351 nm [33]. These higher energy transitions were caused by the pyridyl units, whereas the lower energy transitions, including the transition at 351 nm, originated from the pyrenyl moiety. This result was found to be in contrast to that of the bisimine complexes of Re^{+}, which tend to be brightly colored because of metal-to-ligand charge-transfer transitions at ca 360 nm [26, 31]. Weak absorption bands were also observed at 267 and 347 nm, which were attributed to a charge-transfer transition and π–π* transitions, respectively. The absorption bands at approximately 329 and 344 nm were blue shifted in the case of **1**, and the absorption intensity became stronger compared with that of the ligand. However, the absorption bands were red shifted in the case of **2**, and the absorption intensity weakened compared with that of the ligand.

Description of crystal structures

Single-crystal X-ray analysis revealed that **L** crystallized in the triclinic space group *P-1* and that its asymmetric unit contained one ligand molecule and two ClO_4^- anions (Fig. 3a). Each ligand molecule made head-to-head contact with another ligand molecule through a weak π–π stacking interaction with a distance of 4.913 Å (Fig. 3b). In addition, each ClO_4^- anion was connected to three other ligand molecules through weak C–H···O hydrogen bonding interactions (i.e., C_7–H_7···O_1: 2.58 Å, C_7–H_7···O_7: 2.57 Å, C_{19}–H_{19}···O_9: 2.55 Å and C_{21}–H_{21}···O_6: 2.54 Å). These interactions led to the formation of a 3D supramolecular structure (Fig. 4).

Compound **1** crystallized in the triclinic space group P-1 and its asymmetric unit contained one Cu^{2+} ion, one ligand, one MeCN molecule as a terminal group and two ClO_4^- counter anions (Fig. 5). The Cu^{2+} was found to be five coordinate to three N atoms from the ligand (i.e., Cu-N_1 2.020(2) Å, Cu-N_2 1.978(2) Å and Cu-N_3 1.979(2) Å), one N atom from the MeCN guest molecule (Cu-N_4

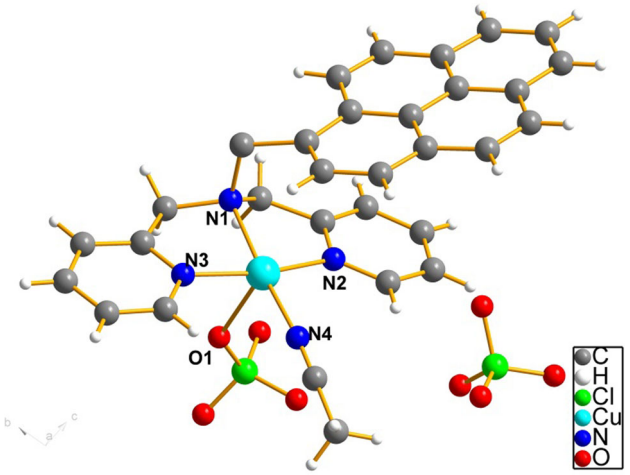

Fig. 5 The asymmetric unit of the compound **1**

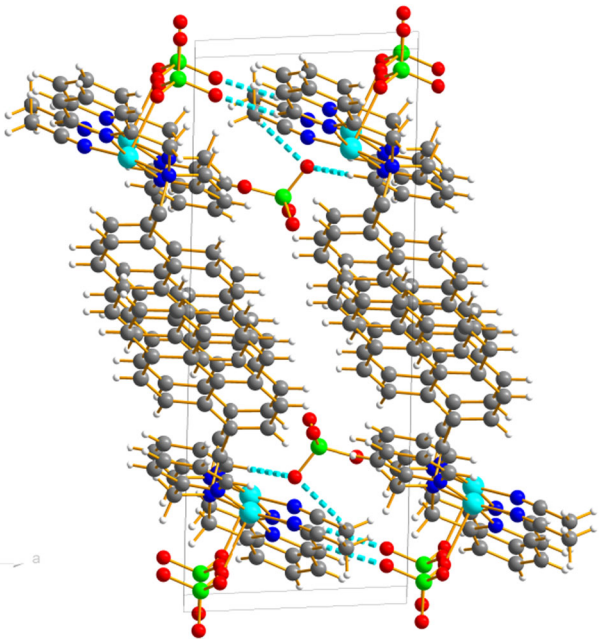

Fig. 7 The hydrogen bonds in **1**

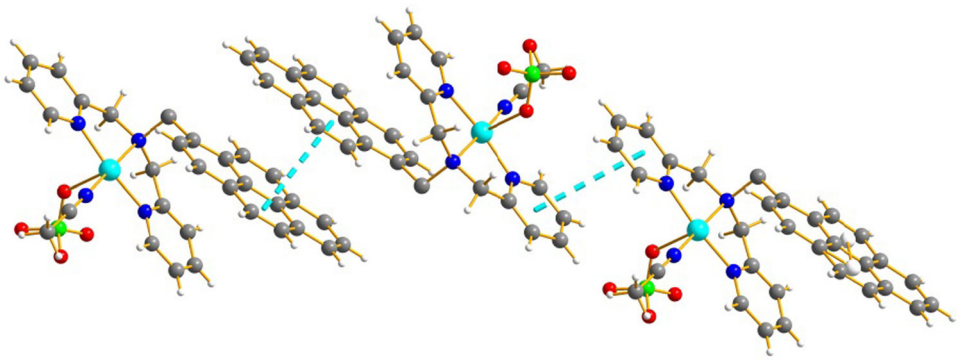

Fig. 6 The weak π…π stacking interactions in compound **1**

1.983(3) Å) and one O atom from the ClO_4^- anion (Cu–O 2.389(2) Å) (Table S2†).

In addition, each asymmetric unit interacted with another unit through a weak π–π stacking interaction between the pyrene and the pyridine rings at distances of 3.905(6) and 4.232(5) Å, respectively (Fig. 6). Furthermore, the ClO_4^- anion combined two asymmetric units via the formation of two weak hydrogen bonding interactions (i.e., C_{21}–$H_{26}\cdots O_4$: 2.519 Å, C_{29}–$H_{29}\cdots O_8$: 2.477 Å, C_{31}–$H_{31B}\cdots O_8$: 2.596 Å), which lead to the formation of a 3D supramolecular structure (Fig. 7).

Compound **2** also crystallized in the triclinic space group *P*–1 and its asymmetric unit contained one Pt(II) ion, one ligand, one coordinated chloride ion and one guest PF_6^- anion (Fig. 8). The Pt(II) center was four-coordinate to the two N atoms from the two pyridine rings of the ligand with Pt–N bond lengths of Pt–N(2) 2.0031(3) Å and Pt–N(3) 2.0057(3) Å, one N atom from the amine nitrogen with a Pt–N bond length of Pt–N(1) 2.0316(3) Å and one

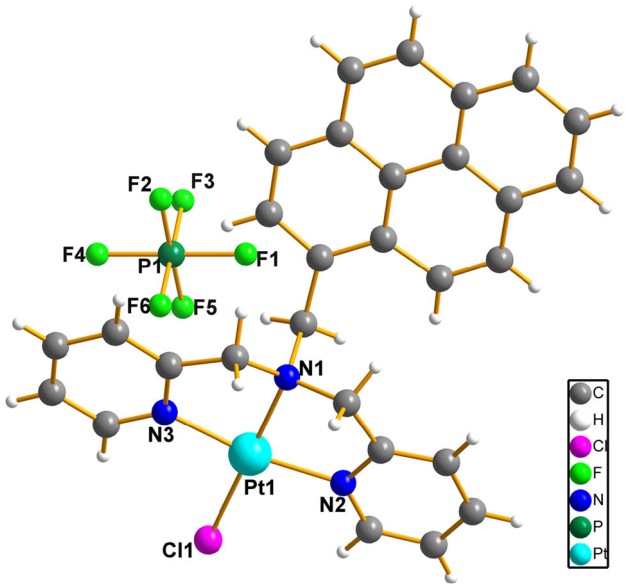

Fig. 8 Molecular structure of **2** with thermal ellipsoids at 45 % probability

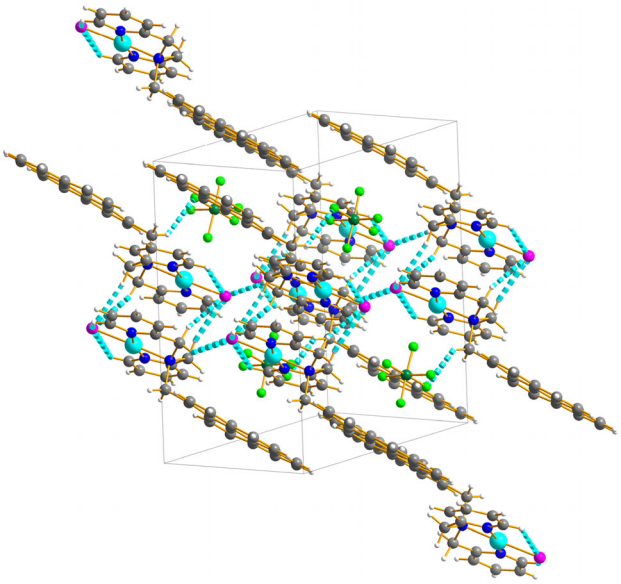

Fig. 10 The hydrogen bond interaction in compound **2** (a-axis projection)

Table 1 In vitro antimicrobial activities (MIC, μg/mL) of **L**, **1** and **2**

Compounds	*E. coli* (ATCC-25922)	*S. aureus* (ATCC-25923)	*C. albicans* (ATCC-10213)
L	NA	NA	NA
1	83.33	166.67	NA
2	10.42	NA	5.43

In each case triplicate tests were performed and the average was taken as the final reading. Values given as μg/mL for all three compounds

MIC minimum inhibitory concentration, *NA* not activity

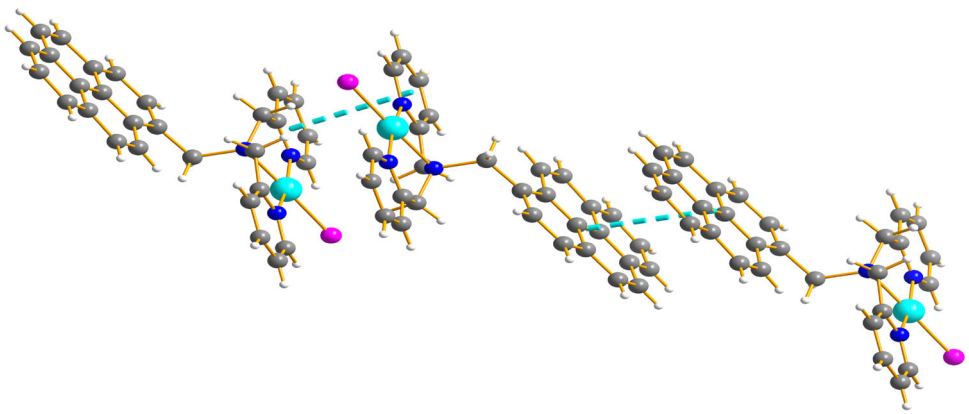

Fig. 9 The π–π interaction between aromatic rings in **2**

coordinated chloride ion with the Pt–Cl bond length of Pt–Cl(1) 2.3014(1) Å (Table S4†).

In addition, the pyrene and pyridine moieties of one molecule of **2** were arranged head-to-tail with the pyrene and pyridine moieties of another molecule of **2**, respectively, and these head-to-tail aggregations were offset in a face-to-face mode at distances of 3.5800 and 3.7813 Å, respectively. These results also suggested that there was a weak π–π stacking interaction between the aromatic rings in compound **2** (Fig. 9). Furthermore, the molecular structures extended into a 3D supramolecular architecture through π–π stacking and hydrogen bonding interactions between the carbon atoms of the pyridine ring and coordinate interactions between the Cl atoms and the F atoms of the PF_6^- anion (Table S8† and Fig. 10).

In vitro antimicrobial assay

The in vitro antimicrobial activities of **L**, **1** and **2** were evaluated against a Gram-positive bacterium (*S. aureus*, CGMCC-1.1477), a Gram-negative bacterium (*E. coli*, ATCC-25922) and a fungus (*C. albicans*, ATCC-10213) were tested, and the results are shown in Table 1. The results show that compounds **1** and **2** exhibited higher activities than the ligand alone. This higher level of activity could be attributed to the formation of chelates, which would reduce the polarity of the metal ions, as well as making them more lipophilic. An increase in the lipophilicity of the chelate would lead to an improvement in the interactions between the compounds and the cell constituents, which would enable them to interfere more effectively with normal cell processes [34]. The data in Table 1 show that the MIC values of compound **1** were 83.33 and 166.67 μg/mL for the wild type Gram-negative and Gram-positive strains of *E. coli* and *S. aureus*, respectively. Compound **2** exhibited a higher level of activity against the Gram-negative bacteria than compound **1**. Unfortunately, however, the Gram-positive bacterium (*S. aureus*) was insensitive to the compound **2**, although compound **2** did show excellent activity towards *C. albicans* with an MIC value of 5.43 μg/mL. Metal ions can play an important role in antimicrobial activity, and we believe that the disparity between the antimicrobial activities of these compounds towards the microorganisms tested in the current study reflects the changes in the bond characteristics of the different metal ions to the target microorganisms because of the molecular structure of the ligand in these compounds are otherwise identical. These compounds are therefore worthy of further research.

Conclusions

We have designed and successfully synthesized two new Cu(II) and Pt(II)-containing compounds, and solved the crystal structures of these compounds using single-crystal XRD. The results of single-crystal XRD analysis showed that the two compounds **1**, **2** were mononuclear, 0D structures, which were further connected through a series of hydrogen bonding interactions into 3D supramolecular architectures. The ligand (**L**) did not exhibit any antimicrobial activity, but its Cu(II) and Pt(II) compounds (compound **1** and **2**) were found to be potential antimicrobial agents. Compound **1** could therefore be used as a new candidate for the treatment of *S. aureus* and *E. coli* infections, and compound **2** could be used as a candidate for the treatment of *E. coli* and *C. albicans* infections. These compounds could help in the discovery of new chemical classes of antimicrobial matter that could serve as selective agents against specific infectious diseases.

Acknowledgments This work was supported by the National Natural Science Foundation of China (21172037 and 81360471), the international cooperation project of Guizhou province (No. [2012]7036), the 'Chunhui' Plan project of Ministry of Education. (No. Z2014089) and the Natural Science Foundation of Fujian, China (Grant No. 2011J01040) for financial support.

References

1. William, M.M., Martin, O.O., Abram, M.M., Morounke, S.: Antitumor activity of phenylene bridged binuclear bis(iminoquinolyl)palladium(II) and platinum(II) complexes. Bioorg. Med. Chem. Lett. **24**, 1692–1694 (2014)
2. Yang, S.N., Shi, W., Xing, D., Zhao, Z., Lv, F.P., Yang, L.P., Yang, Y.S., Hu, W.H.: Synthesis, antibacterial activity, and biological evaluation of formyl hydroxyamino derivatives as novel potent peptide deformylase inhibitors against drug-resistant bacteria. Eur. J. Med. Chem. **86**, 133–152 (2014)
3. Thorsteinn, L.: Self-assembled cyclodextrin nanoparticles and drug delivery. J. Incl. Phenom. Macrocycl. Chem. **80**, 1–7 (2014)
4. Singh, D.P., Ramesh, K., Surain, P., Aneja, K.R.: Spectroscopic and antimicrobial studies of macrocyclic metal complexes derived from 1,8-diaminonaphthalene and dimedone. J. Incl. Phenom. Macrocycl. Chem. **78**, 363–369 (2014)
5. Trevor, W.H.: Developing new metal-based therapeutics: challenges and opportunities. Dalton Trans. **36**, 4929–4937 (2007)
6. Wang, X.Y., Guo, Z.J.: Targeting and delivery of platinum-based anticancer drugs. Chem. Soc. Rev. **42**, 202–224 (2013)
7. Una, B., Vesna, L., Vesna, V., Milica, B., Zoran, M., Suzana, D.: Copper nanoparticles with high antimicrobial activity. Mater. Lett. **128**, 75–78 (2014)
8. Andrew, D.K., Thomas, E.H., Jason, E.B., Dzung, C.T., Yngard, R., Eddie, L.C.: Differential effects of Co(III), Ni(II), and Ru(III) amine complexes on Sindbis virus. J. Inorg. Biochem. **104**, 592–598 (2010)
9. Sreedaran, S., Bharathi, K.S., Rahiman, A.K., Jagadish, L., Kaviyarasan, V., Narayanan, V.: Synthesis, electrochemical, magnetic, catalytic and antimicrobial studies of N-functionalized cyclam based trinuclear copper(II) and nickel(II) complexes. J. Incl. Phenom. Macrocycl. Chem. **66**, 297–306 (2010)
10. Zimmerman, J.R., de Bettencourt-Dias, A.: Homobinuclear sulfato-bridged and mononuclear nitrato complexes of Cu(II) with

thiophen-2-yl-dipicolylamine; structure and anion-dependent absorption spectra. Inorg. Chem. Commun. **14**, 753–758 (2011)
11. Antonioli, B., Buchner, B., Clegg, J., Gloe, K.K., Gotzke, L., Heine, A., Jager, A., Jolliffe, K.A., Kataeva, O., Kataev, V., Klingeler, R., Krause, T., Lindoy, L.F., Popa, A., Seichter, W., Wenzel, M.: Interaction of an extended series of N-substituted di(2-picolyl)amine derivatives with copper(II). Synthetic, structural, magnetic and solution studies. Dalton Trans. **38**, 4795–4805 (2009)
12. Natarajan, R., Narayanaperumal, P.: DNA fastening and ripping actions of novel Knoevenagel condensed dicarboxylic acid complexes in antitumor. Eur. J. Med. Chem. **80**, 57–70 (2014)
13. Frederick, F.B., Bimal, K.B.: Polycyclic aromatic compounds as anticancer agents: synthesis and biological evaluation of some chrysene derivatives. Bioorg. Med. Chem. Lett. **8**, 2877–2880 (1998)
14. Chen, X.Q., Wang, J.Y., Zhang, T.Y., Zhang, L.Z., Peng, X.J.: Synthesis and DNA cleavage activity of diiron(III) complex bearing pyrene group. Chin. Chem. Lett. **19**, 342–344 (2008)
15. Michele, B.P., Daniela, B., Francesco, P., Lisa, L., Marta, V., Carlo, P., Francesco, Q., Giuseppe, R.: Induction of brown cells in *Venerupis philippinarum* exposed to benzo(a)pyrene. Fish. Shellfish Immunol. **40**, 233–238 (2014)
16. Banik, B.K., Becker, F.F.: Polycyclic aromatic compounds as anticancer agents: structure–activity relationships of chrysene and pyrene derivatives. Bioorg. Med. Chem. **9**, 593–605 (2001)
17. Kamal, A., Ramesh, G., Srinivas, O., Ramulu, P.: Synthesis and antitumour activity of pyrene-linked pyrrolo [2,1-c] and benzodiazepine hybrids. Bioorg. Med. Chem. **14**, 471–474 (2004)
18. Uttara, B., Imran, K., Akhtar, H., Paturu, K., Akhil, R.: C.: photodynamic effect in near-IR light by a photocytotoxic iron(III) cellular imaging agent. Angew. Chem. Int. Ed. **51**, 2658–2661 (2012)
19. Yuan, Z.L., Yang, X.Q., Wang, L., Huang, J.D., Wei, G.: Efficient synthesis of new asymmetric tripodal ligands using microwave irradiation, and their crystal structures. RSC Adv. **4**, 42211–42214 (2014)
20. Yuan, Z.L., Hu, Q.H., Wu, Q., Zhang, M.Q., Zhu, B.X.: Synthesis and antibacterial activity of novel Schiff base macrocyclic compounds. Chin. J. Org. Chem. **29**, 279–282 (2009)
21. Yuan, Z.L., Wu, Q., Yang, X.B., Hu, Q.H., Zhang, M.Q.: Synthesis and antibacterial activity of novel Schiff base macrocyclic compounds containing triazole. Chin. J. Org. Chem. **31**, 1698–1702 (2011)
22. Bratsos, I., Mitri, E., Ravalico, F., Zangrando, E., Gianferrara, T., Bergamo, A., Alessio, E.: New half sandwich Ru(II) coordination compounds for anticancer activity. Dalton Trans. **41**, 7358–7371 (2012)
23. CrystalClear, version 1.36, Molecular Structure Corp and Rigaku Corp., The Woodlands, TX, and Tokyo, Japan (2000)
24. Sheldrick G. M.: SHELXS 97, program for crystal structure solution; University of Göttingen, Göttingen
25. Nitis, C.S., Susmita, M., Mousumi, D., Nasima, K., Debmalya, M., Amalesh, S., Slawin, A.M.Z., Ray, J., Butcher, R.S.: Synthesis characterization, X-ray crystallography and antimicrobial activities of new Co(III) and Cu(II) complexes with a pyrazole based Schiff base ligand. Polyhedron **68**, 122–130 (2014)
26. Sarker, S.D., Nahar, L., Kumarasamy, Y.: Microtitre plate-based antibacterial assay incorporating resazurin as an indicator of cell growth, and its application in the in vitro antibacterial screening of phytochemicals. Methods **42**, 321–324 (2007)
27. Geary, W.J.: The use of conductivity measurements in organic solvents for the characterisation of coordination compounds. Coord. Chem. Rev. **7**, 81–86 (1971)
28. Saptarshi, B., Subrata, N., Michael, G.B.D., Carolina, E., Antonio, F., Ashutosh, G.: Trinuclear and tetranuclear adduct formation between sodium perchlorate and copper(II) complexes of salicylaldimine type ligands: structural characterization and theoretical investigation. Inorg. Chim. Acta **366**, 219–226 (2011)
29. Forel, M.T., Tranquille, M.: Spectres de vibration du diméthylsulfoxyde et dn diméthylsulfoxyde-d_6. Spectrochim. Acta **26A**, 1023–1034 (1970)
30. Yuan, Z.L., Zhang, Q.L., Liang, X., Zhu, B.X., Lindoy, L.F., Wei, G.: A new series of dinucleating macrocyclic ligands and their complexes of zinc(II). Polyhedron **27**, 344–348 (2008)
31. Neville, S.N., Peter, L., David, E.H., Yang, Q.F., Jerikho, C.B., Wu, M.J., Janice, R.A.W.: The antimicrobial properties of some copper(II) and platinum(II) 1,10-phenanthroline complexes. Dalton Trans. **42**, 3196–3209 (2013)
32. Anup, N.K., Anupa, A.K., Ayesha, A.K., Pranaya, V.J., Vedavati, G.P.: Monitoring cellular uptake and cytotoxicity of copper(ii) complex using a fluorescent anthracene thiosemicarbazone ligand. Bioconjug. Chem. **25**, 102–114 (2014)
33. Lucy, A.M., Rebecca, H.L., Lindsay, P.H., Niklaas, J.B., Simon, J.A.P.: Rhenium complexes of chromophore-appended dipicolylamine ligands: syntheses, spectroscopic properties, DNA binding and X-ray crystal structure. New J. Chem. **32**, 2140–2149 (2008)
34. Liu, H.H., Yang, W., Zhou, W.Q., Xu, Y.L., Xie, J., Li, M.Y.: Crystal structures and antimicrobial activities of copper(II) complexes of fluorine-containing thioureido ligands. Inorg. Chim. Acta **405**, 387–394 (2013)